IL NUOVO CIMENTO **47 C** (2024) 5
DOI 10.1393/ncc/i2024-24005-4

Colloquia: La Thuile 2023

Rare and semileptonic decays and LFNU at LHCb

P. K. Resmi(*)
Department of Physics, University of Oxford - Oxford, UK

received 10 October 2023

Summary. — The couplings of electroweak gauge bosons and the different lepton families are universal in the Standard Model. However, recent measurements have shown deviations from this behavior, which could potentially be due to contribution from new physics. The lepton flavour universality tests done at the LHCb experiment using tree-level and rare B decays, lepton flavour violating decays and decay rate measurements of some rare decays are presented.

1. – Introduction

The Standard Model (SM) is lepton flavour universal, *i.e.*, the couplings between electroweak gauge bosons and the different lepton families are universal and any difference between the interactions of e, μ and τ is driven only by the difference in their mass. The lepton flavour universality (LFU) is tested by measuring the ratios of branching fractions of decays involving different leptons [1]. Such ratios are ideal experimental probes since the uncertainties related to form factor normalizations mostly cancel and could be sensitive to a possible enhanced coupling to the third generation [2,3].

The LFU ratios are constructed in tree-level semileptonic decays of the type $b \to c\ell\nu_\ell$ as

$$R(X_c) = \frac{\mathcal{B}(X_b \to X_c \tau^+ \nu_\tau)}{\mathcal{B}(X_b \to X_c \ell \nu_\ell)}, \tag{1a}$$

where $X_b = B^0, B^+_{(c)}, B^0_s, \Lambda_b, ...$ and $X_c = D, D^*, J/\psi, D_s, \Lambda_c, ...$ are hadrons with b and c quarks, respectively. The ratios

$$R_{K^*} = \frac{\mathcal{B}(B^0 \to K^{*0}\mu^+\mu^-)}{\mathcal{B}(B^0 \to K^{*0}e^+e^-)} \tag{2a}$$

$$R_K = \frac{\mathcal{B}(B^+ \to K^+\mu^+\mu^-)}{\mathcal{B}(B^+ \to K^+e^+e^-)} \tag{2b}$$

(*) On behalf of the LHCb Collaboration

could be constructed for loop-level rare decays of the type $b \to s\ell\ell$.

Rare decays, as the name suggests, have a small branching fraction ($\leq 10^{-4}$) in the SM and the transitions are flavour-changing neutral currents (FCNC). Any enhancements in the decay rates would also point towards new physics beyond the SM. Lepton flavour violating decays like $b \to s\ell\ell'$ and decays of the type $c \to u\ell\ell$ can also provide similar insights.

The LFU ratio measurements in both semileptonic and rare decays along with other recent measurements involving rare decays performed at LHCb are presented here.

2. – Tree-level semileptonic decays

Semileptonic decays involving $b \to c\ell\nu_\ell$ transitions have been exploited to measure various LFU ratios $R(X_c)$ by both B-factories (Belle and BaBar) and LHCb. The average of the combination of measurements of the ratios $R(D)$ and $R(D^*)$ is more than 3σ away from the SM prediction [1]. Therefore, it is important to have more precise measurements to understand this discrepancy better. These measurements are challenging because neutrinos in the final states are not detected and kinematic approximations are needed to reconstruct the parent X_b hadron.

Two sets of τ^+ decays are considered while looking at LFU ratios at LHCb: muonic decays as $\tau^+ \to \mu^+\nu_\mu\bar{\nu}_\tau$ and hadronic decays as $\tau^+ \to \pi^+\pi^-\pi^+(\pi^0)\bar{\nu}_\tau$. With muonic decays, the $R(X_c)$ ratios can be measured directly since the numerator and denominator decays are both accessible with the same visible final state. Hadronic τ^+ decays would require external inputs for branching fractions of the normalisation modes in order to obtain $R(X_c)$. However, the sample purity is better than that in muonic decays with good control over the background components. Measurements with both of these τ^+ decays would also provide an internal consistency check.

The ratio $R(D^*)$ has been measured using both the τ^+ modes [4, 5]. Some of the $R(X_c)$ ratios are uniquely accessible at LHCb like $R(J/\psi)$ and $R(\Lambda_c)$. The former is measured using muonic τ^+ decays [6] while the latter with the hadronic counterpart [7]. These measurements are carried out using the Run 1 data sample corresponding to an integrated luminosity of 3 fb^{-1} at centre of mass energies $\sqrt{s} = 7, 8$ GeV collected during 2011–2012. There are new updates to both the $R(D^*)$ measurements and they are summarized below.

2˙1. *$R(D^{(*)})$ with muonic τ^+ decays.* – The $R(D^*)$ measurement with muonic τ^+ decays have been updated into a simultaneous extraction of $R(D)$ and $R(D^*)$ [8]. Samples are selected with $D^0\mu$ and $D^*\mu$ candidates with the D^0 and D^* decays as $D^0 \to K^-\pi^+$ and $D^{*+} \to D^0\pi^+$, respectively. The selection has been improved with a custom μ identification classifier which is flatter in kinematic acceptance. This reduces the misidentification background, which was the dominant systematic uncertainty in the previous $R(D^*)$ measurement [4]. Trigger selection is based on D^0 so that the acceptance is preserved for low momentum muons. The $D^0\mu$ sample is five times larger than the $D^*\mu$ sample.

The yields of the signal mode $B \to D^{(*)}\tau\nu$ and normalisation mode $B \to D^{(*)}\mu\nu$ are determined from a three-dimensional binned template fit to the variables $q^2 \equiv (p_B - p_{D^{(*)}})^2$, $m^2_{\text{mass}} \equiv (p_B - p_{D^{(*)}} - p_\mu)^2$ and muon energy E^*_μ, where p_X is the four-momentum of particle X. The fit projections are shown in fig. 1. The largest background contribution comes from partially reconstructed B decays like $B \to D^{**}\mu\nu$ and $B \to D^{*(*)}D^{(*)}(\to$

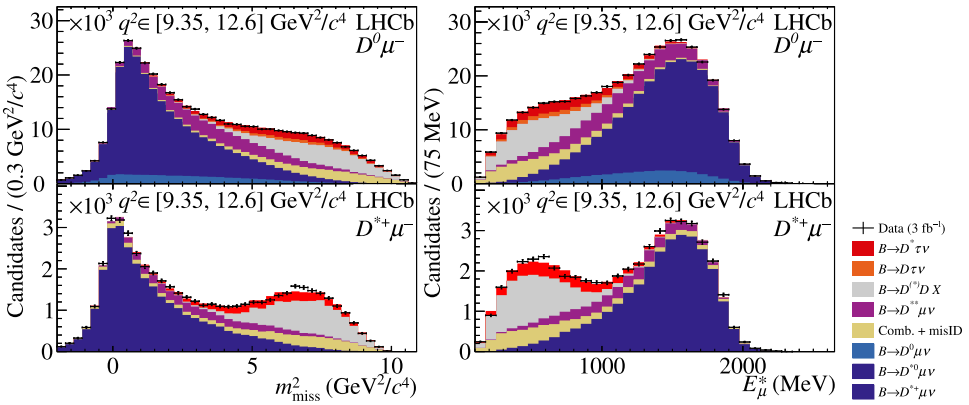

Fig. 1. – Distributions of $m^2_{\rm miss}$ (left) and $E^*_{\mu^+}$ (right) in the specified q^2 bins of the signal data, overlaid with projections of the fit model with all normalization and shape parameters at their best-fit values.

$\mu X)X$. The results are

$$R(D) = 0.441 \pm 0.060 \pm 0.066 \tag{3a}$$

$$R(D^*) = 0.281 \pm 0.018 \pm 0.023, \tag{3b}$$

where the first uncertainty is statistical and second is systematic. They agree with the SM expectations at 1.9σ significance.

2˙2. $R(D^{(*)})$ *with hadronic* τ^+ *decays.* – $R(D^*)$ with three-prong hadronic τ^+ decays is measured as $R(D^*) = \mathcal{K}(D^*)\frac{\mathcal{B}(B^0\to D^{*-}3\pi^\pm)}{\mathcal{B}(B^0\to D^{*-}\mu\nu_\mu)}$, where $\mathcal{K}(D^*) = \frac{\mathcal{B}(B^0\to D^{*-}\tau^+\nu_\tau)}{\mathcal{B}(B^0\to D^{*-}3\pi^\pm)}$ has been measured and the other branching fractions form external input [9]. The normalisation mode, $B^0 \to D^{*-}3\pi^\pm$, has the same visible final state as that of the signal mode. The τ decay vertex is reconstructed from the three charged pion daughter candidates.

The LHCb hadronic $R(D^*)$ analysis was first performed using the Run 1 sample [5], corresponding to an integrated luminosity of 3 fb^{-1}. This is updated with additional pp collision data taken at 13 TeV in 2015 and 2016, corresponding to an integrated luminosity of 2 fb^{-1} [9]. Despite the lower integrated luminosity, the increase of the $b\bar{b}$ production cross section with the centre-of-mass energy by nearly a factor of two and improvements in the LHCb trigger provide about 40% more signal candidates than in the previous analysis.

The dominant background is coming from $B \to D^{*-}3\pi^\pm X$ decays, where the charged pions originate directly from the B meson. They are suppressed by requiring the τ vertex to be downstream with respect to the B vertex along the beam direction. This detachment criteria along with a multivariate classifier that utilises more vertex separation variables, reject more than 99% of these backgrounds.

The largest remaining backgrounds in the selected data sample are $B \to D^*DX$ decays or double-charm decays where $D = D_s, D^+, D^0$. They mimic the signal topology due to the non-negligible life time of the charm mesons. The dominant contributions come from $D_s \to 3\pi X$ decays whereas D^+ and D^0 decays form sub-leading contributions. A multivariate boosted-decision-tree (BDT) classifier is used to separate D_s decays from

signal τ decays. The differences in the kinematics and resonant structure of both types of decays are exploited.

A three-dimensional binned template fit is used to extract the signal yield, with the variables $q^2 \equiv (p_{B^0} - p_{D^*})^2$, τ^+ decay time, and the output of BDT trained to discriminate τ from D_s. The background templates need to be modelled correctly and the simulation samples used should reflect data conditions as much as possible. This is achieved by correcting the simulation samples for any differences found from data control sample studies. A sample enriched in D_s decays is obtained by reversing the anti-D_s BDT selection. This is used to study the decay of D_s into $3\pi X$ final state. The branching fractions of various such decays are determined from a simultaneous binned maximum-likelihood fit in the data sample to the distribution of four variables: $\min[m(\pi^+\pi^-)]$, $\max[m(\pi^+\pi^-)]$, $m(\pi^+\pi^-)$, which represents the reconstructed masses of all possible two-pion combinations of the candidate, and $m(3\pi)$. The simulation is corrected to reflect the resulting branching fraction values obtained from the fit.

The relative abundance of different $B \to D^* D_s X$ decays provides important constraints in the signal fit. These relative fractions are determined from a fit to the data control sample enriched in $B \to D^* D_s(\to 3\pi)X$ decays. The selection of the control sample differs from the default selection by requiring the 3π mass to be within 20 MeV/c^2 of the known D_s mass An extended binned maximum-likelihood fit is performed to the distribution of the difference of the $D^{*-}3\pi$ mass and the sum of the reconstructed $\bar{D}^0$ and 3π masses, *i.e.*, $m(D^{*-}3\pi) - m(\bar{D}^0) - m(3\pi)$. The obtained fractions are used as Gaussian constraints in the signal extraction fit.

There are 2469 ± 154 candidates of $B^0 \to D^{*-}\tau^+\nu_\tau$ decays obtained from the signal fit. The fit projections are shown in fig. 2. The dominant systematic uncertainty comes from the modelling of double charm background decays. There are about 30,000 normalisation mode $B^0 \to D^{*-}3\pi^\pm$ decays as obtained from an unbinned maximum likelihood fit to $m(D^{*-}3\pi^\pm)$. These yields and the efficiencies are used to determine $\kappa(D^*)$, yielding a result of $1.70 \pm 0.10^{+0.11}_{-0.10}$, where the uncertainties are statistical and systematic, respectively. The improved analysis procedure results in an increase in signal efficiency and a decrease of the relative systematic uncertainty from 9% to 6%. Using the most recent branching fraction measurements $B^0 \to D^{*-}3\pi^\pm = (7.21 \pm 0.29) \times 10^{-3}$ and $B^0 \to D^{*-}\mu^+\nu_\mu = (4.97 \pm 0.12)\%$ [10], the branching fraction

$$\mathcal{B}(B^0 \to D^{*-}\tau^+\nu_\tau) = (1.23 \pm 0.07^{+0.08}_{-0.07} \pm 0.05) \times 10^{-2}\,,$$

and the ratio of branching fractions of $B^0 \to D^{*-}\tau^+\nu_\tau$ and $B^0 \to D^{*-}\mu^+\nu_\mu$

$$R(D^*) = 0.247 \pm 0.015 \pm 0.015 \pm 0.012\,,$$

are obtained, where the third uncertainties are due to the uncertainties on the external branching fractions. When combined with the previous results [5], the value $R(D^*)$ is

$$R(D^*)_{\rm comb} = 0.257 \pm 0.012 \pm 0.014 \pm 0.012\,.$$

This combination leads to one of the most precise measurements of $R(D^*)$ to date. When these results are included, the $R(D) - R(D^*)$ combination is still in tension with the SM prediction at more than 3σ significance [1].

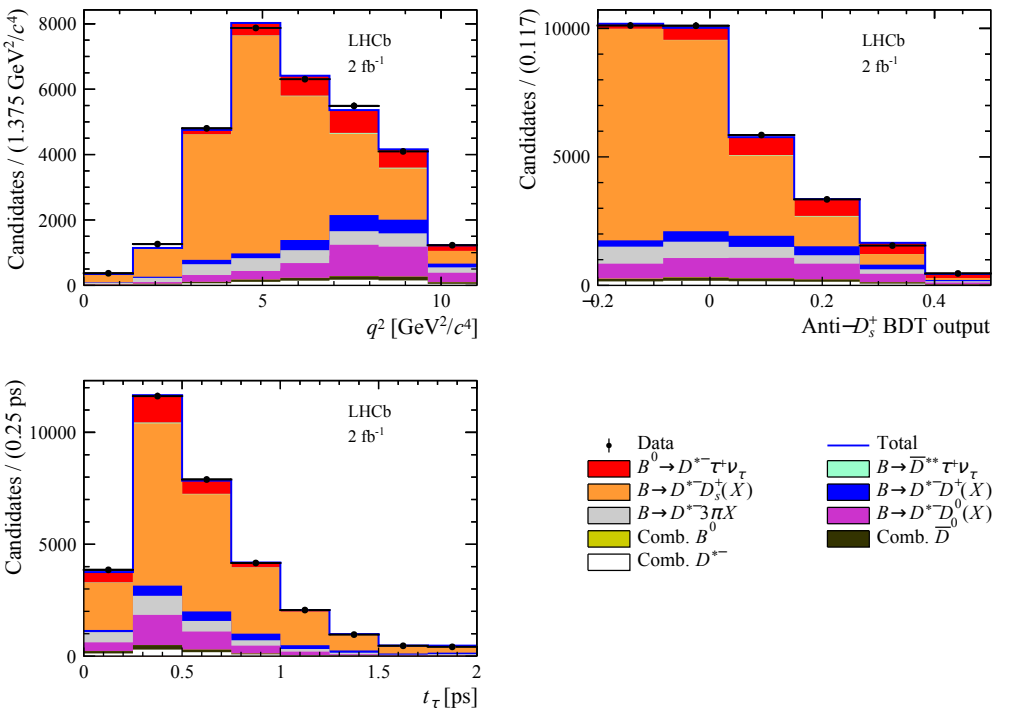

Fig. 2. – Distributions of q^2 (top left), BDT output (top right) and τ decay time (bottom left) of the signal data, overlaid with projections of the fit model with all normalization and shape parameters at their best-fit values

3. – Rare decays

Flavour changing neutral current transitions such as $b \to s\ell\ell$ are suppressed in the SM making them a powerful probe for new physics. Several tensions with the SM predictions are seen in branching fractions and angular observables in these rare decays [11]. The largest theoretical uncertainities are contributions from hadronic effects. However, such uncertainties mostly cancel out in ratios of branching fractions, so that they are precisely predicted, $R_H = \frac{\mathcal{B}(H_B \to H\mu^+\mu^-)}{\mathcal{B}(H_B \to He^+e^-)} = 1.00 \pm 0.01$ [12].

The double ratios $R_{K^{(*)}} = \frac{\mathcal{B}(B \to K^{(*)}\mu^+\mu^-)}{\mathcal{B}(B \to K^{(*)}e^+e^-)} \Big/ \frac{\mathcal{B}(B \to J/\psi(\mu^+\mu^-)K^{(*)})}{\mathcal{B}(B \to J/\psi(e^+e^-)K^{(*)})}$ are measured at LHCb to gain better control of the efficiency with the help of the control mode ($B \to J/\psi K^{(*)}$) that is expected to be lepton universal even in the presence of new physics [13]. This ensures the cancellation of most of the experimental systematic contributions to the measurements. The measurements are done in the non-resonant region, $1.1 < q^2 < 6.0$ GeV^2, where q^2 is the dilepton invariant mass-squared.

The presence of electrons in the final state poses more challenges in the reconstruction at LHCb. Since they are light in mass, they interact with the detector material through bremsstrahlung emission, leading to a poor momentum resolution compared to any other charged particles. This energy loss is recovered in the reconstruction with a non negligible inefficiency by correcting the electron momentum with the energy of a photon in the

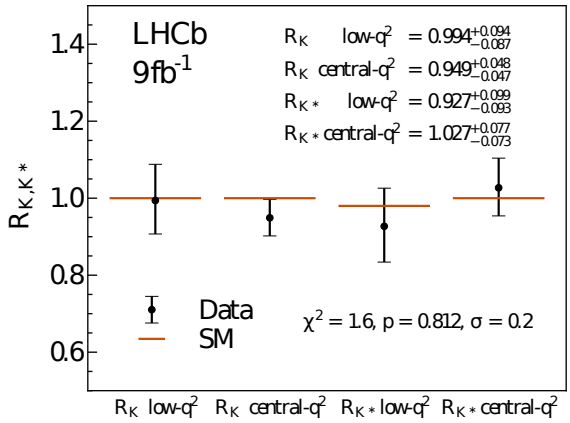

Fig. 3. – Results of R_K and R_{K^*} in regions of q^2.

calorimeter that is compatible with the electron direction.

A simultaneous measurement of the ratios R_K and R_{K^*} is carried out based on the full LHCb dataset corresponding to an integrated luminosity of 9 fb^{-1} [14, 15]. This is done in two regions of q^2: low [0.1–1.1] GeV$^2/c^2$ and central [1.1–6.0] GeV$^2/c^2$, which are sensitive to contributions from the different Wilson coefficients. A simultaneous maximum likelihood fit to the B mass distribution for the muon and electron modes is used to extract the ratio observable. The results are shown in fig. 3 and they agree with the SM expectations within 1σ.

Other rare decays that are forbidden in the SM are also good probes to look for new physics beyond the SM. Lepton flavour violating decays of the type $b \to s\ell\ell'$ and baryon number violating decays $B^0_{(s)} \to p\mu^-$ are searched for at LHCb using the full Run 1 and Run 2 data sample. No signal is observed for any of the decay modes [16-18]. More FCNC decays are also being searched for including $D^0 \to \mu^+\mu^-$ and $K^0_{\rm S,L} \to 4\mu$ [19, 20]. Upper limits are set at 90% confidence level. These are summarised in table I.

TABLE I. – *Upper limits set at 90% confidence level for the rare FCNC decays.*

Mode	Limit
$B^0 \to K^{*0}\mu^\pm e^\mp$	10.1×10^{-9}
$B^0_s \to \phi\mu^\pm e^\mp$	16.0×10^{-9}
$B^0 \to K^{*0}\tau^+\mu^-$	1.0×10^{-5}
$B^0 \to K^{*0}\tau^-\mu^+$	8.2×10^{-6}
$B^0 \to p\mu^-$	2.6×10^{-9}
$B^0_s \to p\mu^-$	12.1×10^{-9}
$D^0 \to \mu^+\mu^-$	3.1×10^{-9}
$K^0_{\rm S} \to \mu^+\mu^-\mu^+\mu^-$	5.1×10^{-12}
$K^0_{\rm L} \to \mu^+\mu^-\mu^+\mu^-$	2.3×10^{-9}

4. – Conclusion and outlook

There are several tensions with the SM predictions observed in the behaviour of leptons in B decays. There are tensions up to 3σ found in measurements involving $b \to c\ell\nu_\ell$ decays. The global picture of $R(D) - R(D^*)$ combination is largely unchanged with the addition of new measurements having tensions with SM at the level of 3σ.

New measurements and observables are needed to understand the nature of these discrepancies and identify the possible sources of new physics, if any. The Run 3 data taking at LHCb has started during which the LHCb detector is expected to collect data corresponding to an integrated luminosity of 25 fb^{-1}. Also thanks to improved trigger and reconstruction techniques, this will allow to make more precise measurements and to explore many new observables, thus helping to further understand the nature of leptons within the SM and beyond.

REFERENCES

[1] Heavy Flavour Averaging Group (Amhis Y. *et al.*), *Eur. Phys. J. C*, **81** (2021) 226.
[2] Fajfer S., Kamenik J. F. and Nišandžić I., *Phys. Rev. D*, **85** (2012) 094025.
[3] Fajfer S. and Nišandžić I., *Phys. Lett. B*, **755** (2016) 270.
[4] LHCb Collaboration (Aaij R. *et al.*), *Phys. Rev. Lett.*, **115** (2015) 111803.
[5] LHCb Collaboration (Aaij R. *et al.*), *Phys. Rev. Lett.*, **120** (2018) 171802.
[6] LHCb Collaboration (Aaij R. *et al.*), *Phys. Rev. Lett.*, **120** (2018) 121801.
[7] LHCb Collaboration (Aaij R. *et al.*), *Phys. Rev. Lett.*, **128** (2022) 191803.
[8] LHCb Collaboration (Aaij R. *et al.*), arXiv:2302.02886 (submitted to *Phys. Rev. Lett.*).
[9] LHCb Collaboration (Aaij R. *et al.*), *Phys. Rev. D.*, **108** (2023) 012018.
[10] Particle Data Group (Workman R. L. *et al.*), *Prog. Theor. Exp. Phys.*, **2022** (2022) 083C01.
[11] LHCb Collaboration (Aaij R. *et al.*), *Phys. Rev. Lett.*, **125** (2020) 011802.
[12] Descotes-Genon S., Hofer L., Matias J. and Virto J., *J. High Energy Phys.*, **2016** (2016) 92.
[13] BESIII Collaboration (Ablikim M. *et al.*), *Phys. Rev. D.*, **88** (2013) 032007.
[14] LHCb Collaboration (Aaij R. *et al.*), *Phys. Rev. Lett.*, **131** (2023) 051803.
[15] LHCb Collaboration (Aaij R. *et al.*), *Phys. Rev. D*, **108** (2023) 032002.
[16] LHCb Collaboration (Aaij R. *et al.*), *J. High Energy Phys.*, **06** (2023) 073.
[17] LHCb Collaboration (Aaij R. *et al.*), *J. High Energy Phys.*, **06** (2023) 143.
[18] LHCb Collaboration (Aaij R. *et al.*), *Phys. Rev. D*, **108** (2023) 012021.
[19] LHCb Collaboration (Aaij R. *et al.*), *Phys. Rev. Lett.*, **131** (2023) 041804.
[20] LHCb Collaboration (Aaij R. *et al.*), *Phys. Rev. D*, **108** (2023) L031102.